# COMPARISON OF EXPERIMENTAL AND ANALYTICAL RESULTS OF VIBRATION OF A FULL SCALE PILE

Kōji Mizuhata (I)
Kaoru Kusakabe (II)
Presenting Author: Koji Mizuhata

## SUMMARY

This paper presents comparison between the analytical results and the experimental results of the full sized pile-ground system having a softer zone around the pile under the action of the horizontal harmonic forces on its head. In the analytical model, it is assumed that the pile is a circular steel pipe and its surrounding softer zone is viscoelastic and that the ground outside of the softer zone consists of three dimensional viscoelastic thin sliced layers. The experiment was conducted on a man-made sand fill island. The results are discussed from the view point of the effect of the softer zone on the frequency characteristics.

## INTRODUCTION

Recently in Japan, many buildings with pile foundations are constructed in the reclaimed or sand fill man-made islands. In these islands, due to pretty large settlement of the ground, the negative skin friction acts on the surface of the end bearing pile. In order to reduce the negative skin friction, bitumen is often coated on the suface of the pile. However, the coated bitumen is easily torn off during pile driving. Therefore, a pile is driven so as to make small clearance between the bitumen and soil and the clearance is filled with sand after or during driving. This method of construction loosens soil around the pile and the resistance of the soil against the vertical and the horizontal forces acting on the pile is weakened during earthquake. Then, in this paper, the horizontal vibration of the pile having the softer zone surrounding its surface is treated analytically and experimentally. This kind of problem was treated previously by Novak et al.(Ref. 1) on the vertical vibration. But they did not deal with the horizontal vibration. In this study the results are discussed from the view point of the effect of the softer zone on the frequency characteristics of the amplitude and the phase difference of the pile in the horizontal vibration. The analytical results are compared with the experimental results of the actual steel pipe pile driven into the sand fill man-made island.

## ANALYTICAL MODEL AND ASSUMPTIONS

The analytical model used in this study is shown in Fig. 1, where an end bearing pile of radius $R_1$ is surrounded by the softer medium of radius $R_2$ and the original ground exists outside of the softer medium and a rigid mass is attached on the head of the pile. In this paper, the softer medium is denoted Zone I and the surrounding ground is Zone II. In the analysis, the models of the pile, the softer medium and the ground are sliced into L horizontal layers

(I) Professor of Structural Eng., Kobe University, Kobe, Japan

(II) Associate Professor of Structural Eng., Kobe University, Kobe, Japan

and the Finite Element Method is used in the vertical direction and the wave theory is used in the horizontal direction. The horizontal excitation is applied to the rigid mass.

The following assumptions are made in the analysis:

(1) Circumference of the pile remains circular during vibration.
(2) The pile is vertical and viscoelastic, and behaves as Timoshenko beam.
(3) The media of both zones in each layer are homogeneous, isotropic and viscoelastic. The layered media overlie a rigid bed rock.
(4) Displacement in each thin layer element varies linearly along depth.
(5) The pile contacts perfectly with the soft medium of Zone I, which does to the ground of Zone II.
(6) The bottom of the pile is clamped with the rigid bed rock.

## EQUATIONS OF MOTION AND SOLUTIONS FOR THE GROUND

For each thin layer element, the equations of motion in cylindrical coordinates are expressed as

$$\left.\begin{aligned}
&(\lambda^*+2\mu^*)\frac{\partial\Theta}{\partial r}-\frac{2\mu^*}{r}\frac{\partial\tilde{\omega}_z}{\partial\theta}+2\mu^*\frac{\partial\tilde{\omega}_\theta}{\partial z}=\rho\frac{\partial^2 u_r}{\partial t^2}\\
&(\lambda^*+2\mu^*)\frac{1}{r}\frac{\partial\Theta}{\partial\theta}-2\mu^*\frac{\partial\tilde{\omega}_r}{\partial z}+2\mu^*\frac{\partial\tilde{\omega}_z}{\partial r}=\rho\frac{\partial^2 u_\theta}{\partial t^2}\\
&(\lambda^*+2\mu^*)\frac{\partial\Theta}{\partial z}-\frac{2\mu^*}{r}\frac{\partial(r\tilde{\omega}_\theta)}{\partial r}+\frac{2\mu^*}{r}\frac{\partial\tilde{\omega}_r}{\partial\theta}=\rho\frac{\partial^2 u_z}{\partial t^2}
\end{aligned}\right\} \quad \cdots (1)$$

where $\lambda^*=\lambda+i\lambda'$, $\mu^*=\mu+i\mu'$, $\lambda$, $\mu$ : Lame's constants, $\lambda'$, $\mu'$ : viscous constants, $\{u_r, u_\theta, u_z\}$ : displacement vector, and

$$\left.\begin{aligned}
&\Theta=\frac{1}{r}\frac{\partial(ru_r)}{\partial r}+\frac{1}{r}\frac{\partial u_\theta}{\partial\theta}+\frac{\partial u_z}{\partial z}\\
&2\tilde{\omega}_r=\frac{1}{r}\frac{\partial u_z}{\partial\theta}-\frac{\partial u_\theta}{\partial z},\qquad 2\tilde{\omega}_\theta=\frac{\partial u_r}{\partial z}-\frac{\partial u_z}{\partial r},\qquad 2\tilde{\omega}_z=\frac{1}{r}\frac{\partial(ru_\theta)}{\partial r}-\frac{1}{r}\frac{\partial u_r}{\partial\theta}
\end{aligned}\right\} \quad \cdots (2)$$

In the case that the head of the pile is excited in the horizontal direction, for symmetry the solutions of Eq. (1) are written by

$$u_r=v_r\cos\theta\, e^{i\omega t},\qquad u_\theta=v_\theta\sin\theta\, e^{i\omega t},\qquad u_z=v_z\cos\theta\, e^{i\omega t} \quad \cdots (3)$$

where

$$\left.\begin{aligned}
v_r=&\sum_{R=1}^{2L}\tfrac{1}{2}(\phi-\psi)_{1R}\{H_2^{(1)}(\kappa_R r)-H_0^{(1)}(\kappa_R r)\}S_R^1+\sum_{R=1}^{2L}\tfrac{1}{2}(\phi-\psi)_{1R}\{H_2^{(2)}(\kappa_R r)-H_0^{(2)}(\kappa_R r)\}S_R^2\\
&+\sum_{S=1}^{L}\tfrac{1}{2}(\phi+\psi)_{1S}\{H_2^{(1)}(\kappa_S r)+H_0^{(1)}(\kappa_S r)\}S_S^1+\sum_{S=1}^{L}\tfrac{1}{2}(\phi+\psi)_{1S}\{H_2^{(2)}(\kappa_S r)+H_0^{(2)}(\kappa_S r)\}S_S^2\\
v_\theta=&\sum_{R=1}^{2L}\tfrac{1}{2}(\phi-\psi)_{1R}\{H_2^{(1)}(\kappa_R r)+H_0^{(1)}(\kappa_R r)\}S_R^1+\sum_{R=1}^{2L}\tfrac{1}{2}(\phi-\psi)_{1R}\{H_2^{(2)}(\kappa_R r)+H_0^{(2)}(\kappa_R r)\}S_R^2\\
&+\sum_{S=1}^{L}\tfrac{1}{2}(\phi+\psi)_{1S}\{H_2^{(1)}(\kappa_S r)-H_0^{(1)}(\kappa_S r)\}S_S^1+\sum_{S=1}^{L}\tfrac{1}{2}(\phi+\psi)_{1S}\{H_2^{(2)}(\kappa_S r)-H_0^{(2)}(\kappa_S r)\}S_S^2\\
v_z=&\sum_{R=1}^{2L}\chi_{1R}H_1^{(1)}(\kappa_R r)S_R^1+\sum_{R=1}^{2L}\chi_{1R}H_1^{(2)}(\kappa_R r)S_R^2
\end{aligned}\right\} \quad \cdots (4)$$

and $e^{i\omega t}$: time function, $\omega$: circular frequency, $\kappa_R$, $\kappa_S$: eigenvalues with respect to the wave numbers of the thin layer, $\phi-\psi$, $\chi$: eigenvectors for $\kappa_R$, $\phi+\psi$: eigenvector for $\kappa_S$, $H_\nu^{(1)}(\kappa r)$, $H_\nu^{(2)}(\kappa r)$: Hankel function of the $\nu$th order of the first and the second kinds, respectively, $S_R^1$, $S_R^2$, $S_S^1$, $S_S^2$: unknown constants. The solutions of Eq.(4) are obtained for both zones and the suffices I and II are attached to the left side of $v_r$, $v_\theta$, and $v_z$ for each zones.

The boundary conditions for the assumption (5) are expressed as follows:

$$\left.{}_{\mathrm{I}}u_r\right|_{r=R_2}={}_{\mathrm{II}}u_r\Big|_{r=R_2},\quad {}_{\mathrm{I}}\lambda_{\mathrm{I}}\Theta+2{}_{\mathrm{I}}\mu\frac{\partial\,{}_{\mathrm{I}}u_r}{\partial r}\Big|_{r=R_2}={}_{\mathrm{II}}\lambda_{\mathrm{II}}\Theta+2{}_{\mathrm{II}}\mu\frac{\partial\,{}_{\mathrm{II}}u_r}{\partial r}\Big|_{r=R_2}$$

$$\left.\begin{aligned} {}_{I}u_{\theta}\big|_{r=R_2} &= {}_{II}u_{\theta}\big|_{r=R_2}, \quad {}_{I}\mu\left(\frac{1}{r}\frac{\partial {}_{I}u_z}{\partial\theta}+\frac{\partial {}_{I}u_{\theta}}{\partial z}\right)_{r=R_2} = {}_{II}\mu\left(\frac{1}{r}\frac{\partial {}_{II}u_z}{\partial\theta}+\frac{\partial {}_{II}u_{\theta}}{\partial z}\right)_{r=R_2} \\ {}_{I}u_{z}\big|_{r=R_2} &= {}_{II}u_{z}\big|_{r=R_2}, \quad {}_{I}\mu\left(\frac{\partial {}_{I}u_r}{\partial z}+\frac{\partial {}_{I}u_z}{\partial r}\right)_{r=R_2} = {}_{II}\mu\left(\frac{\partial {}_{II}u_r}{\partial z}+\frac{\partial {}_{II}u_z}{\partial r}\right)_{r=R_2} \end{aligned}\right\} \quad \cdots (5)$$

When the displacements on the circumference of the pile are expressed by $V_{r1}$, $V_{\theta 1}$, and $V_{z1}$, the assumption (1) yields

$$ {}_{I}v_r(r,z_1)=V_{r1}, \qquad {}_{I}v_{\theta}(r,z_1)=V_{\theta 1}, \qquad {}_{I}v_z(r,z_1)=V_{z1} \qquad \cdots (6)$$

When the number of the thin layer element is L, the number of the unknown constant $S_2$ defined by Eq.(4) is 2L for ${}_{I}S^{1}_{R}$, 2L for ${}_{I}S^{2}_{R}$, L for ${}_{I}S^{2}_{S}$, L for ${}_{I}S^{1}_{S}$, 2L for ${}_{II}S^{2}_{R}$, L for ${}_{II}S^{2}_{S}$ and 9L in total. Herein, the unknowns, ${}_{II}S^{1}_{R}$ and ${}_{II}S^{1}_{S}$, in Zone II correspond to the back-going wave and are excluded, because the waves radiate infinitely and are not reflected. On the other hand, the number of equations for the boundary conditions is 6L for Eq.(5), 3L for Eq.(6) and 9L in total. However, 3L of displacements are unknown. Eqs. (5) and (6) are expressed in matrix representation as

$$[H]\{S\} = \{V\} \qquad \cdots (7)$$

where
$$\{V\} = (V_r \; V_{\theta 1} \; V_z \; 0 \; 0 \; 0 \; 0 \; 0 \; 0)^T \qquad \cdots (8)$$
$$\{S\} = ({}_{I}S^{1}_{R} \; {}_{I}S^{1}_{S} \; {}_{I}S^{2}_{R} \; {}_{I}S^{2}_{S} \; {}_{II}S^{2}_{R} \; {}_{II}S^{2}_{S})^T$$

$$\{S\} = [H]^{-1}\{V\} \qquad \cdots (9)$$

The stresses on the circumference of the pile are expressed as

$$\begin{Bmatrix} \sigma_r \\ \tau_{r\theta} \\ \tau_{rz} \end{Bmatrix}_{r=R_1} = -\begin{bmatrix} \cos\theta & 0 & \\ & \sin\theta & \\ 0 & & \cos\theta \end{bmatrix}\begin{Bmatrix} p_r \\ p_{\theta} \\ p_z \end{Bmatrix} \qquad \cdots (10)$$

In the case that displacements are expressed by Eqs. (3) and (4), the stresses $p_r$, $p_{\theta}$, $p_z$ are written as

$$\begin{aligned} p_r &= -\left[{}_{I}\lambda\left\{\frac{1}{r}\frac{\partial}{\partial r}(rv_r)+\frac{v_{\theta}}{r}+\frac{\partial v_z}{\partial z}\right\}+2\,{}_{I}\mu\frac{\partial v_r}{\partial r}\right]_{r=R_1} \\ &= \sum_R\left\{\frac{2\,{}_{I}\mu}{R_1}(\phi-\psi)\,{}_{1R}H^{(1)}_2(\kappa_R R_1)-({}_{I}\lambda+2\,{}_{I}\mu)(\phi-\psi)\,{}_{1R}\kappa_R H^{(1)}_1(\kappa_R R_1)-{}_{I}\lambda\frac{\partial \chi_{1R}}{\partial z}H^{(1)}_1(\kappa_R R_1)\right\}{}_{I}S^{1}_{R} \\ &\quad +\sum_R\left\{\frac{2\,{}_{I}\mu}{R_1}(\phi-\psi)\,{}_{1R}H^{(2)}_2(\kappa_R R_1)-({}_{I}\lambda+2\,{}_{I}\mu)(\phi-\psi)\,{}_{1R}\kappa_R H^{(2)}_1(\kappa_R R_1)-{}_{I}\lambda\frac{\partial \chi_{1R}}{\partial z}H^{(2)}_1(\kappa_R R_1)\right\}{}_{I}S^{2}_{R} \\ &\quad +\sum_S\frac{2\,{}_{I}\mu}{R_1}(\phi+\psi)\,{}_{1S}H^{(1)}_2(\kappa_S R_1)\,{}_{I}S^{1}_{S}+\sum_S\frac{2\,{}_{I}\mu}{R_1}(\phi+\psi)\,{}_{1S}H^{(2)}_2(\kappa_S R_1)\,{}_{I}S^{2}_{S} \end{aligned} \qquad (11)$$

$$\begin{aligned} p_{\theta} &= -{}_{I}\mu\left(\frac{\partial v_{\theta}}{\partial r}-\frac{v_{\theta}}{r}-\frac{v_r}{r}\right)_{r=R_1} \\ &= \sum_R\frac{2\,{}_{I}\mu}{R_1}(\phi-\psi)\,{}_{1R}H^{(1)}_2(\kappa_R R_1)S^{1}_{R}+\sum_R\frac{2\,{}_{I}\mu}{R_1}(\phi-\psi)\,{}_{1R}H^{(2)}_2(\kappa_R R_1)S^{2}_{R} \\ &\quad +\sum_S\left\{\frac{2\,{}_{I}\mu}{R_1}(\phi+\psi)\,{}_{1S}H^{(1)}_2(\kappa_S R_1)-{}_{I}\mu(\phi+\psi)\,{}_{1S}\kappa_S H^{(1)}_1(\kappa_S R_1)\right\}{}_{I}S^{1}_{S} \\ &\quad +\sum_S\left\{\frac{2\,{}_{I}\mu}{R_1}(\phi+\psi)\,{}_{1S}H^{(2)}_2(\kappa_S R_1)-{}_{I}\mu(\phi+\psi)\,{}_{1S}\kappa_S H^{(2)}_1(\kappa_S R_1)\right\}{}_{I}S^{2}_{S} \end{aligned} \qquad (12)$$

$$\begin{aligned} p_z &= -{}_{I}\mu\left(\frac{\partial v_r}{\partial z}+\frac{\partial v_z}{\partial r}\right)_{r=R_1} \\ &= -\sum_R\frac{{}_{I}\mu}{2}\left\{\frac{\partial}{\partial z}(\phi-\psi)\,{}_{1R}-\chi_{1R}\kappa_R\right\}\left\{H^{(1)}_2(\kappa_R R_1)-H^{(1)}_0(\kappa_R R_1)\right\}{}_{I}S^{1}_{R} \\ &\quad -\sum_R\frac{{}_{I}\mu}{2}\left\{\frac{\partial}{\partial z}(\phi-\psi)\,{}_{1R}-\chi_{1R}\kappa_R\right\}\left\{H^{(2)}_2(\kappa_R R_1)-H^{(2)}_0(\kappa_R R_1)\right\}{}_{I}S^{2}_{R} \\ &\quad -\sum_S\frac{{}_{I}\mu}{2}\frac{\partial}{\partial z}(\phi+\psi)\,{}_{1S}\left\{H^{(1)}_2(\kappa_S R_1)+H^{(1)}_0(\kappa_S R_1)\right\}{}_{I}S^{1}_{S} \\ &\quad -\sum_S\frac{{}_{I}\mu}{2}\frac{\partial}{\partial z}(\phi+\psi)\,{}_{1S}\left\{H^{(2)}_2(\kappa_S R_1)+H^{(2)}_0(\kappa_S R_1)\right\}{}_{I}S^{2}_{S} \end{aligned} \qquad (13)$$

The assumption (4) yields

$$\left.\begin{aligned}\phi &= \phi_1\left(\frac{1}{2}-\frac{z}{h}\right)+\phi_2\left(\frac{1}{2}+\frac{z}{h}\right)\\ \psi &= \psi_1\left(\frac{1}{2}-\frac{z}{h}\right)+\psi_2\left(\frac{1}{2}+\frac{z}{h}\right) \qquad -\frac{h}{2}\le z\le\frac{h}{2}\\ \chi &= \chi_1\left(\frac{1}{2}-\frac{z}{h}\right)+\chi_2\left(\frac{1}{2}+\frac{z}{h}\right)\end{aligned}\right\} \quad \cdots (14)$$

Stresses distributing on the upper and the lower boundaries of the l-th layer element are expressed in matrix representation as

$$\{p\}=\begin{Bmatrix}p_r\\ p_\theta\\ p_z\end{Bmatrix}=[D]\{S_0\} \qquad \{S_0\}=({}_IS_R^1\ {}_IS_R^2\ {}_IS_S^1\ {}_IS_S^2)^T \quad \cdots (15)$$

Forces and bending moment acting on the pile at the boundary between the pile and soil in the l-th layer are expressed as

$$\left.\begin{aligned}p_{\chi l} &= \int_{-\pi}^{\pi}\{p_{rl}\cos\theta\cos\theta-p_{\theta l}\sin\theta\sin\theta\}R_l\,d\theta=\pi R_l(p_{rl}-p_{\theta l})\\ p_{\theta l} &= \int_{-\pi}^{\pi}p_{zl}\cos\theta R_l\,d\theta=0\\ m_{yl} &= \int_{-\pi}^{\pi}p_{zl}\cos\theta R_l\cos\theta R_l\,d\theta=\pi R_l^2p_{zl}\end{aligned}\right\} \quad \cdots (16)$$

Eq. (15) is expressed by the unknown displacement as

$$\{p\}=[D]\{S_0\}=[D][\bar{H}]\{V_0\}=[Y]\{V_0\} \quad \cdots (17)$$

where $[\bar{H}]$ is a submatrix of the inverse matrix of $[H]$, that is,

$$[H]^{-1}=\begin{bmatrix}\boxed{\bar{H}} & \\ & \end{bmatrix}, \qquad \{V\}=\begin{Bmatrix}V_0\\ 0\\ 0\end{Bmatrix}$$

By Eq. (16), Eq. (17) is shrunk as

$$\{P\}=\pi[R][T]^T[Y][T]\{V\} \quad \cdots (18)$$

where

$$[T]^T=\begin{bmatrix}I_L & -I_L & O_L\\ I_L & O_L & I_L\end{bmatrix}, \qquad [R]=\begin{bmatrix}R_1 & 0\\ 0 & R_1\end{bmatrix}, \qquad \{V\}=(V_r,V_z)^T \quad \cdots (19)$$

and $I_L$ is a unit matrix of L×L, and $O_L$ is a null matrix of L×L.

## EQUATIONS OF MOTION FOR THE PILE

The pile is regarded as the Timoshenko beam, where the reaction force by the surrounding soil acts on the pile. The equations of motion for the combined shear and bending vibration of the pile is written, for each thin layer element, as

$$\left.\begin{aligned}&\frac{\partial}{\partial z}\left[\kappa_t G^*A\left(\frac{\partial u'}{\partial z}+\frac{w'}{R}\right)\right]=\rho A\frac{\partial^2u'}{\partial t^2}\\ &\frac{\partial}{\partial z}\left(\frac{E^*I}{R}\frac{\partial w'}{\partial z}\right)-\kappa_t G^*A\left(\frac{\partial u'}{\partial z}+\frac{w'}{R}\right)=\frac{\rho I}{R}\frac{\partial^2w'}{\partial t^2}\end{aligned}\right\} \quad \cdots (20)$$

where A, I: cross-sectional area and moment of inertia of the pile, respectively, R: radius of the pile, $\rho$: density of the pile, $E^*$, $G^*$: complex moduli of rigidity of the pile, respectively, $\kappa_t$: shape factor for shear and 0.85 for circular cross-section. Herein, under the assumption (4), the mass matrix M and the rigidity matrix F on the upper and the lower boundaries of each thin element of the pile can be obtained by the principle of virtual work and the equation of motion for the pile is written as

$$([F]+[P]-\omega^2[M])\{V\}=\{Q\} \quad \cdots (21)$$

where [F]: rigidity matrix of the pile, [P]: reaction force of the soil acting on the circumference of the pile, [M]: mass matrix of the pile, {V}: displacement vector of the pile, and [Q]: external disturbance applied to the pile. In Eq.(20), u' and w' are the displacements of the pile.

## NUMERICAL ANALYSIS

As a standard model for the numerical analysis, the following rigid mass-pile-soil system is adopted under the consideration of the experiment: The pile is a straight steel pipe pile with the closed end of 38.7m in length, 65cm in diameter (neglecting the slip layer) and 14mm (3.7m of the upper part) and 10mm (35m of the lower part) in thickness. Density, Young's modulus and the shear modulus of the pile are 7.86g/cm$^3$, 2100t/cm$^2$, and 810t/cm$^2$, respectively. The damping constant G'/G is assumed to be 0.001, where G*=G+iG'. The rigid mass made of concrete of 2m×2m in plan and 1m in height and 10t in weight is attached to the head of the pile. The cylindrical elastic medium in Zone I around the pile has the width of 10cm, the density $\rho_I$ of 1.5t/m$^3$, and the shear wave velocity $V_{sI}$ of 210m/sec as the standard values. The ground of Zone II outside of Zone I has the thickness of 38.5m, the density $\rho_{II}$ of 2.0 t/m$^3$, and the shear wave velocity $V_{sII}$ of 210m/sec as the standard values. For both Zone I and Zone II, the square value of the ratio of the shear and the longitudinal wave velocities, $n^2=(V_s/V_p)^2=(1-2\nu)/2(1-\nu)$, of 0.02 is taken and the damping ratio $\eta=V_s\mu'/R_0\mu$ of 0.1 is assumed as the standard values. In order to investigate the effect of softness of the surrounding soil on the amplitude and the phase vs. frequency characteristics, the ratio of the shear wave velocity of the soil in Zone I to that of the ground in Zone II, $n_s = V_{sI}/V_{sII}$, is changed parametrically as shown in Table 1. However, variation of the parameters along depth shown in Table 2 is not changed. The pile and the ground are sliced into 12 and 11 thin elements, respectively.

The numerical results of the analysis are shown in Figs. 4(a), 4(b), 5(a) and 5(b). These figures show the relationship between the amplitude of the velocity of the rigid mass per unit exciting force and the phase difference from resonance and the exciting frequency. Figs. 4(a) and 4(b) are for the horizontal direction and Figs. 5(a) and 5(b) are for the vertical direction in rocking motion. By Figs. 4 and 5, it is recognized that the smaller the velocity ratio $n_s$, that is, the softer the soil around the pile, the lower the resonance frequency and the larger the amplitude.

## EXPERIMENTAL STUDY

Vibration tests of the full-sized sigle steel pipe pile having a rigid concrete mass at its head were carried out at the Kobe Port Island, a man-made island in the Osaka Bay in Japan. Profiles of soil and the pile are shown in Fig. 2. At the test site, soft alluvial clay layers and sandy fill overlie diluvial layers consisting of alternating layers of sandy and cohesive soils. The wave velocities of the ground measured near the test site are shown in Fig. 3. The test pile is a steel pipe pile with open end of 43.2m in length, 65cm (31.2m of the upper part) ∿ 81.2cm (10m of the lower part) in diameter, and 14mm (13.7m of the upper part), 10mm (23m of the middle part and 10m of the lowest part) and 12mm (the rest) in thickness. Circumference of the upper and the middle parts of the pile is coated by bitumen of 6mm in thickness in order to reduce the negative skin friction acting on the pile due to the consolidation settlement of the soft alluvial clay layer by the load of the sandy fill. The pile with enlarged lower portion is effective for preventing segregation of bitumen coating on the pile. However, this kind of pile is generally liable to have less lateral resistance because of a clearance between soil and the upper pile. The test pile was driven into the ground by means of a hydraulic or a diesel hammer after preboring by an earth auger of 31m in depth and 80∿90cm in diameter. The clearance between soil and the pile was filled

with in-situ sand, which makes Zone I. After the test pile was constructed, the rigid concrete mass of 2m, 2m and 1m in width, depth and height, respectively and 9.8tonf in weight was made firmly upon the head of the pile. On the rigid concrete mass, a vibration generator with eccentric rotating mass was installed at the center and four accelerometers of servo-type were set at the mid-point of each sides of the rigid mass. In the vibration test, the harmonic vibration was given the rigid concrete mass in the horizontal direction by means of the vibration generator. Advantages of the vibration generator are to record out the signal expressing the position of the rotating mass and to execute the automatic frequency sweep. The sweeping speed of 0.05∿0.08Hz/sec was adopted, because the reponses to the sweep excitation almost coincide with those to the harmonic one for about 0.08Hz/sec. The eccentric moments and their corresponding frequency ranges in the test were first 6kg·cm in 2∿60 Hz and secondly 30kg·cm in 2∿24Hz. Data processing and the graphic display were done by means of a personal computer together with A/D converters right after each test at the test site. The relationship of the amplitude of the velocity per unit exciting force versus frequency is shown in Figs. 6(a) and 7(a) for 6kg·cm of the eccentric mass moment and in Figs. 8(a) and 9(a) for 30 kg·cm. Also, the relationship of the phase difference of the response from resonance versus exciting frequency is shown in Figs. 6(b) and 7(b) for 6kg·cm and in Figs. 8(b) and 9(b) for 30kg·cm. Figs. 6 and 8 are for the horizontal direction and Figs. 7 and 9 are for the vertical direction due to rocking motion. In Figs. 6∿9, ∘ shows the increasing frequency test and × does the decreasing one. By Figs. 6∿9, it is recognized that the resonance frequency for 6kg·cm is 10Hz, while that for 30kg·cm is 7.5Hz and, also, that the resonance frequency for the increasing frequency test is higher than that for the decreasing one. These phenomena may be because the larger the exciting force, the weaker the soil right around the pile and because of nonlinearity of the constitutive relation of soil. Another resonance frequency is recognized around 50Hz for 6kg·cm. This may be because of the dynamic property of the ground, but the reason is not yet clarified at present.

## COMPARISON OF THE EXPERIMENTAL AND THE ANALYTICAL RESULTS

Although the experimental peak value of the amplitude per unit exciting force is five times as big as the analytical one and the discrepancy is large, the experimental resonance frequency is near the analytical one for $n_s=V_{sI}/V_{sII}=0.1$ and the analytical values of both the amplitude and the frequency at resonance approach to the experimental ones as $n_s$ becomes smaller. However, the shear wave velocity of sand can not be reduced so much. Therefore, the clearance between soil and the upper part of the pile as well as the nonlinear constitutive relation of soil will have to be introduced in the analysis even for 6kg·cm of the eccentric mass moment.

## CONCLUSIONS

In this study, the analytical and the experimental results for the horizontal vibration of the full-sized steel pipe pile driven in the soft sand filled ground have been presented and both results have been compared from the view point of the effect of the softer zone around the pile on the frequency characteristics of the amplitude and the phase difference of the pile. From this study, the followings have been concluded:

(1) As the analytical results, it is obtained that the smaller the wave velocity of the medium of the cylindrical softer zone around the pile, the lower

the resonance frequency and the larger the amplitude.

(2) As the experimental results, it is obtained that the larger the eccentric mass moment, the lower the resonance frequency and that the resonance frequency for the increasing exciting frequency test is higher than that for the decreasing one.

(3) The resonance frequency of the horizontal vibration of the steel pipe pile of 65cm in diameter and 43.2m in length with the rigid concrete mass of 9.8tonf in weight driven in the soft sand fill ground is 7.5∿10Hz.

(4) The experimental peak value of the amplitude of the response is larger than the analytical one, while the experimental resonance frequency is near the analytical one for 0.1 of the ratio of the shear wave velocity of Zone I to that of Zone II. The analytical values of both the amplitude and the frequency at resonance approach to the experimental ones, as $n_s$ becomes small.

REFERENCES


(1) M. Sheta and M. Novak: "Vertical Vibration of Pile Groups", GT Div., Proc. of ASCE., Apr. 1982.

(2) T. Kobori and K. Kusakabe: " Dynamic Cross-Interaction Between Two Embedded Structures", Proc. of 5JEES., Oct., 1978


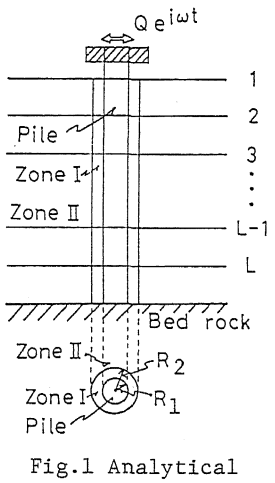


Fig.1 Analytical Model

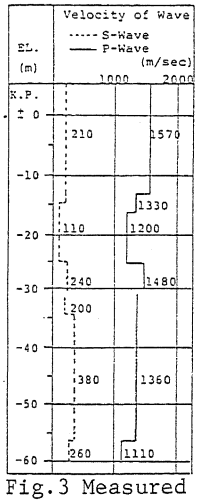


Fig.3 Measured Wave Velocities

Table 1 Combination of Parameters for the Numerical Analysis

| | Zone I | | Zone II | | $n_s$ = |
|---|---|---|---|---|---|
| | $V_{sI}$ m/sec | $\rho_I$ g/cm$^3$ | $V_{sII}$ m/sec | $\rho_{II}$ g/cm$^3$ | $V_{sI}/V_{sII}$ |
| Case 1 | 210 | 1.5 | 210 | 2.0 | 1.0 |
| Case 2 | 105 | 1.5 | 210 | 2.0 | 0.5 |
| Case 3 | 42 | 1.5 | 210 | 2.0 | 0.2 |
| Case 4 | 21 | 1.5 | 210 | 2.0 | 0.1 |

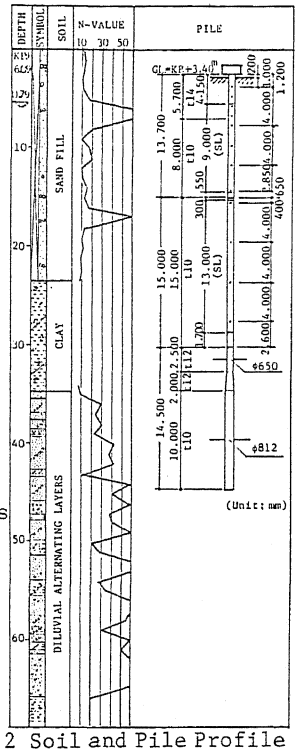


Fig.2 Soil and Pile Profile

Table 2 Variation of Parameters along Depth in the Numerical Analysis

| | Pile | | | | | | Zone I | | | Zone II | | |
|---|---|---|---|---|---|---|---|---|---|---|---|---|
| L | h | $\rho_s$ | G | E | $t_s$ | $n_s$ | $n_I^2$ | $\mu_I$ | $\rho_I$ | $n_{II}^2$ | $\mu_{II}$ | $\rho_{II}$ |
| | 1.20 | 7.86 | 810 | 2100 | 0.014 | 0.001 | | | | | | |
| 1 | 3.50 | 7.86 | 810 | 2100 | 0.014 | 0.001 | 0.02 | 1.0 | 1.0 | 0.02 | 1.0 | 1.0 |
| 2 | 3.50 | 7.86 | 810 | 2100 | 0.010 | 0.001 | 0.02 | 1.0 | 1.0 | 0.02 | 1.0 | 1.0 |
| 3 | 3.50 | 7.86 | 810 | 2100 | 0.010 | 0.001 | 0.02 | 1.0 | 1.0 | 0.02 | 1.0 | 1.0 |
| 4 | 3.50 | 7.86 | 810 | 2100 | 0.010 | 0.001 | 0.02 | 1.0 | 1.0 | 0.02 | 1.0 | 1.0 |
| 5 | 3.50 | 7.86 | 810 | 2100 | 0.010 | 0.001 | 0.02 | 1.0 | 1.0 | 0.02 | 1.0 | 1.0 |
| 6 | 3.50 | 7.86 | 810 | 2100 | 0.010 | 0.001 | 0.02 | 1.0 | 1.0 | 0.02 | 1.0 | 1.0 |
| 7 | 3.50 | 7.86 | 810 | 2100 | 0.010 | 0.001 | 0.02 | 1.0 | 1.0 | 0.02 | 1.0 | 1.0 |
| 8 | 3.50 | 7.86 | 810 | 2100 | 0.010 | 0.001 | 0.02 | 1.0 | 1.0 | 0.02 | 1.0 | 1.0 |
| 9 | 3.50 | 7.86 | 810 | 2100 | 0.010 | 0.001 | 0.02 | 1.0 | 1.0 | 0.02 | 1.0 | 1.0 |
| 10 | 3.50 | 7.86 | 810 | 2100 | 0.010 | 0.001 | 0.02 | 1.0 | 1.0 | 0.02 | 1.0 | 1.0 |
| 11 | 3.50 | 7.86 | 810 | 2100 | 0.010 | 0.001 | 0.02 | 1.0 | 1.0 | 0.02 | 1.0 | 1.0 |

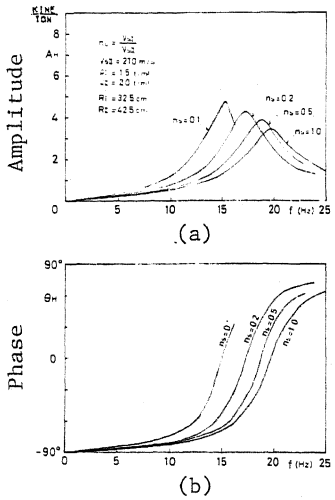


Fig.4 Analytical Results of the Horizontal Velocity

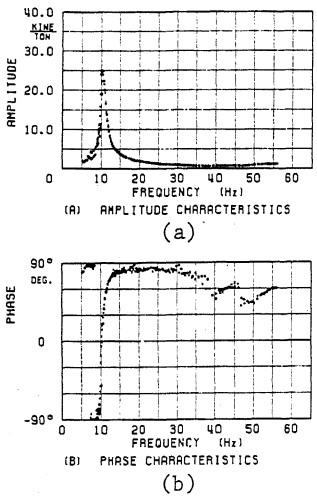


Fig.6 Experimental Results of the Horizontal Velocity for 6kg·cm

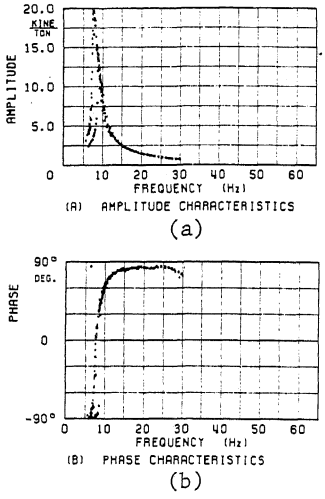


Fig.8 Experimental Results of the Horizontal Velocity for 30kg·cm

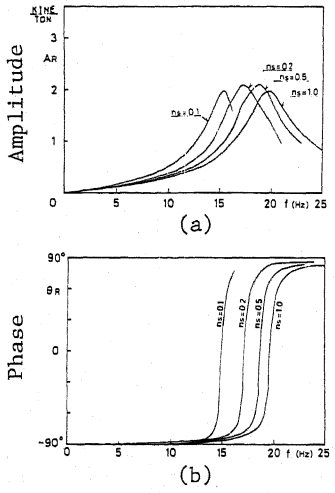


Fig.5 Analytical Results of the Vertical Velocity

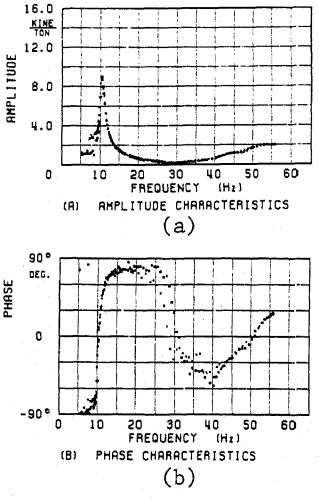


Fig.7 Experimental Results of the Vertical Velocity for 6kg·cm

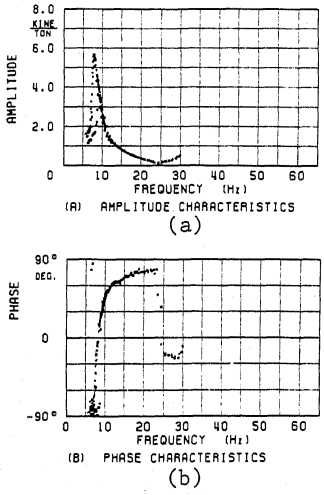


Fig.9 Experimental Results of the Vertical Velocity for 30kg·cm

ACKNOWLEDGEMENT

The authors wish to express their sincere gratitude to Dr. Takuji Kobori, Professor of Kyoto University, for lending the vibration generator. The authors are also indebted to Department of Construction of Kobe City, Showa Sekkei Co. Ltd., Takenaka Komuten Co. Ltd., and Kawasaki Steel Co. Ltd. for providing the test pile and the test site. Thanks are due to the Messrs. Yukinori Maeda, Hisashi Nozoe, Kazuyoshi Katayama and other members of the Earthquake Engineering Laboratory at Kobe University for assisting in the experiment.